Sensor and Simulation Notes

Note 498

April 2005

A Solid Dielectric Lens Impulse Radiating Antenna with High Dielectric Constant Surrounded by a Cylindrical Shroud

Leland H. Bowen and Everett G. Farr
Farr Research, Inc.

J. Scott Tyo and Mustafa Dogan
University of New Mexico

Larry L. Altgilbers
U.S. Army Space and Missile Defense Command

Abstract

We continue here our investigation of Solid Dielectric Lens Impulse Radiating Antennas (SDL IRAs), which are intended for Ultra-Wideband, high-voltage radiation from the front end of an electrically conducting cylindrical shroud. This device is intended to radiate the highest possible field from the smallest possible aperture using the highest possible source voltage. Furthermore, this antenna is intended to be capable of sustaining high g-forces. The antenna consists of a TEM horn embedded into a solid dielectric, with a lens in the aperture at the air-dielectric interface. The antenna is surrounded by an electrically conducting cylindrical shroud that is open at the ends. We extend our earlier work by replacing the polyethylene dielectric material with Kynar® PVDF (PolyVinyliDene Fluoride), which has a dielectric constant of 8.5. Our goal is to improve the low-frequency response of the antenna by making it appear electrically larger. Our investigation includes both numerical modeling of the antenna and experimental measurements. We found the higher dielectric material improved the performance only at very low frequencies, where our measurement technique is approximate. At other frequencies, the performance was either the same or worse than that of an earlier version.

Table of Contents

I. INTRODUCTION.

The objective of this work is to develop an antenna for radiating high-power ultra-wideband (UWB) electromagnetic impulses from extremely compact and durable packages. This objective is based on the need for an antenna that can radiate as broad a bandwidth as possible with maximum gain and at maximum voltage, from as small a package as possible. In addition, the antenna should be rugged enough to tolerate high g-forces.

To meet these objectives, we continue here the development of the Solid Dielectric Lens Impulse Radiating Antenna (SDL IRA) [1, 2]. This device is a lens TEM horn that is fully immersed in dielectric material, contained within an electrically conducting cylindrical shroud that is open at the ends. The dielectric used in [1] was Ultra-High Molecular Weight polyethylene (UHMW), with a dielectric constant of 2.3. In [1], we developed two versions – a 50-ohm (LoZ) version and one with a higher impedance (HiZ). The high-impedance version had the best performance, so we investigate here methods of improving on that design. The major design change is the use of a higher dielectric material to improve the low frequency response of the antenna without increasing the physical size of the antenna [3, 4]. We refer to the new version as the SDL-3.

We begin this paper by describing the design of the SDL-3. For this experiment we used Kynar® PVDF (PolyVinyliDene Fluoride) as the dielectric. Kynar® has a dielectric constant (ε_r) of 8.5 which nearly doubles the electrical size of the antenna without increasing the physical size. Also, several modifications were made with the intent of improving the TDR and the high voltage standoff capability of the device.

Next we show results from numerically modeling the antenna to determine the expected radiation pattern of the antenna. These predictions are compared with test results for the antenna at low voltage. The test results include measurements made with the shroud at 6 different positions with respect to the aperture of the horn. Complete data including TDR, normalized impulse response, gain and antenna patterns are given for the shroud flush with the aperture and 10 cm behind the aperture. Finally we test the antenna at high voltage using a 120 kV Marx generator to verify operation at this voltage.

We begin now with the antenna design.

II. DESIGN.

In [1], we designed and fabricated two versions of a TEM horn immersed in a solid dielectric. The first version was a 50-ohm design for applications requiring low reflections and a matched impedance. The second version was a high-impedance (HiZ) design to maximize realized gain by taking maximum advantage of the available aperture area. From tests on these two antennas, we determined that the HiZ version provided the best impulse response. This is the design that we chose for further development in this effort. However, in this effort, we wish to study the effects of using a higher dielectric constant material for embedding the TEM horn. While a high dielectric material should extend the frequency range at the low end, it may also increase the loss at the high end due to the reflection at the air-dielectric interface.

We selected the high dielectric material Kynar®, with dielectric constant 8.5, to fill our antenna. A list of available materials is shown in Table 2.1 of [1] for the SDL IRA, and we repeat part of this list as Table 2.1 below. The dielectric material used in [1] was ultra-high molecular weight (UHMW) polyethylene which has $\varepsilon_r = 2.3$. Using Kynar® should increase the electrical size of the antenna by a factor of 1.92 ($\sqrt{8.5}/\sqrt{2.3}$) [3]. Note in Table 2.1 that b/a is ratio of the plate separation to plate width in the aperture of the TEM horn. Note also that in Table 2.1 the "gain due to increased aperture area" is an approximation that is calculated from the ratio of the area between the plates for a 50-ohm TEM horn in different dielectric media. Materials with higher dielectric constants have a b/a closer to unity, so they make better use of the aperture.

Table 2.1. Dielectric Material Properties and Calculated Gain.

Material	Dielectric Constant	Dielectric Strength (V/mil)	b/a for 50 Ω	Gain due to increased aperture(dB)	Transmission Coefficient at interface	Loss due to reflection (dB)	Net Relative gain (dB)
Air	1.0		0.17	0.00	1.00	0.00	0.00
UHMW	2.3	2280	0.27	1.9	0.80	2.00	–0.10
Kynar®	8.5	1700	0.70	4.6	0.51	5.84	–1.22

The outer dimensions of the modified SDL-3 are the same as those used in [1]. The TEM horn section of the antenna is embedded within a dielectric cylinder with diameter 12.7 cm (5 in.) and length of 30.5 cm (12 in.). There is a stub at the end of this cylinder to help support the RG-220 coax cable required for high-voltage operation. For the outer housing or shroud we used a standard aluminum tube with outer diameter 15.24 cm (6 in.), wall thickness 1.27 cm (0.5 in.) and length 30.5 cm (12 in.). The length of the TEM horn section is 20.3 cm (8 in.). The aluminum tube is a separate piece that can be moved freely over the antenna, to control the degree to which the antenna protrudes in front of the cylinder or shroud.

The width of the feed elements and their spacing were adjusted to match the 50-ohm impedance of the RG-220 feed cable. The separation between the plates at the feed point is 10.2 mm (0.4 in.); however, there is a point in the transition where the spacing is only about 5 mm (0.198 in.). This spacing should be sufficient to stand off the required high voltage pulse. However, since the dielectric is not continuous (has mating surfaces) in this area, a layer of high quality UHMW is added to help prevent arcing. Also, the surfaces of the Kynar® were coated with a silicone dielectric compound (Dow-DC4) for the high voltage experiments.

The antenna is designed to maintain a 50 Ω impedance up to the junction with the feed elements. We assume here that the impedance of the horn is dominated by the differential mode. We acknowledge the presence of a common mode formed by the two feed elements against the grounded shroud, but our assumption here is that the common mode is excited only weakly. There is a slight mismatch possible at the transition to the feed elements. The taper of the TEM feed is such that the impedance at the feed point is 50 Ω but at the lens the aperture is as large as possible given the restriction of the size of the conductive shroud. At the lens, the aperture is square (86.4 mm X 86.4 mm). The impedance of the TEM feed goes from 50 Ω at the feed to 61 Ω at the aperture. For the UHMW case (HiZ in [1]) the impedance was 117 Ω at the aperture, so we hoped that using the Kynar® would improve both the low-frequency response and the impedance match. It should be noted, however, that there is a large change in the dielectric constant at the lens/air interface that causes a reflection. Also it should be noted that the dielectric constant of most materials trend downward at high frequencies, so the impedance varies somewhat with frequency.

Since we are using a high dielectric material to improve the low frequency response, we calculate the expected low frequency cutoff point and compare it with the UHMW filled antenna. The low end of the frequency response extends down to a frequency, f_L, which is calculated as

$$f_L = \frac{c}{2\pi\sqrt{\varepsilon_r}\,L} \tag{1}$$

where L is the length of the TEM horn, ε_r is the dielectric constant of the filling material, and c is the speed of light in free space. This expression is derived from [5, Equation 4.4], with a modification to include the effect of the dielectric material. Note the apparent advantage in using a high dielectric constant for low-frequency performance. According to this expression, our antenna with a 20.3 cm length and dielectric constant of 8.5 has a low-frequency cutoff frequency of 81 MHz. For the UHMW antennas, we calculated f_L = 155 MHz. These predictions may be optimistic, since the measured data from [1] showed somewhat higher cutoff frequencies.

The new antenna is shown in Figure 2.1 with the shroud in place. To improve performance, we actually positioned the aperture of the antenna in front of the shroud. The antenna with the shroud removed is shown in Figure 2.2. In Figures 2.1 and 2.2 the different sections of Kynar® are shown in different colors (or grayscales) so they can be separated visually. In Figure 2.3 we show an exploded view of the antenna to expose the TEM feed elements and the junction with the coax cable. A photo of the antenna as built is shown in Figure 2.4 with the RG-220 cable attached and with the aluminum shroud in the flush position.

To improve the high-voltage standoff of the antenna, there are two thin sheets, each with a thickness of 0.5 mm (0.020 in.), of high quality (high purity) UHMW between the feed elements. The Kynar® has a dielectric strength of 70 kV/mm (1700 V/mil), which is somewhat lower than the 90 kV/mm (2280 V/mil) for standard UHMW. The high-quality UHMW is expected to have an even higher dielectric strength than the standard variety. The gaps or contact surfaces are all filled or coated with a silicone dielectric compound to help prevent arcing during the high-voltage experiments. The dielectric constant of the silicon grease is about 3.0 and the dielectric strength is about 20 kV/mm (500 V/mil). This dielectric strength is not as high as we would like, however, it should function satisfactorily to prevent arcs from following the surfaces of the Kynar®. Experience has shown that the dielectric strength is much higher for short pulses than for low frequency or DC exposures.

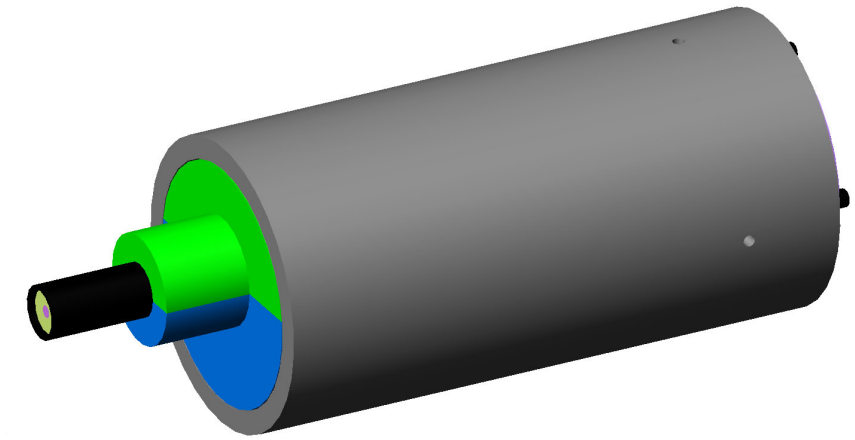

Figure 2.1. SDL-3 with the aluminum shroud in place.

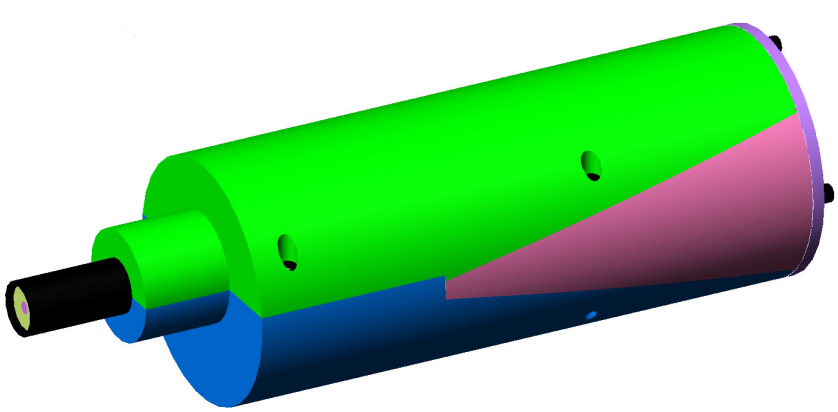

Figure 2.2. SDL-3 with the shroud removed and Kynar® sections shown in different colors.

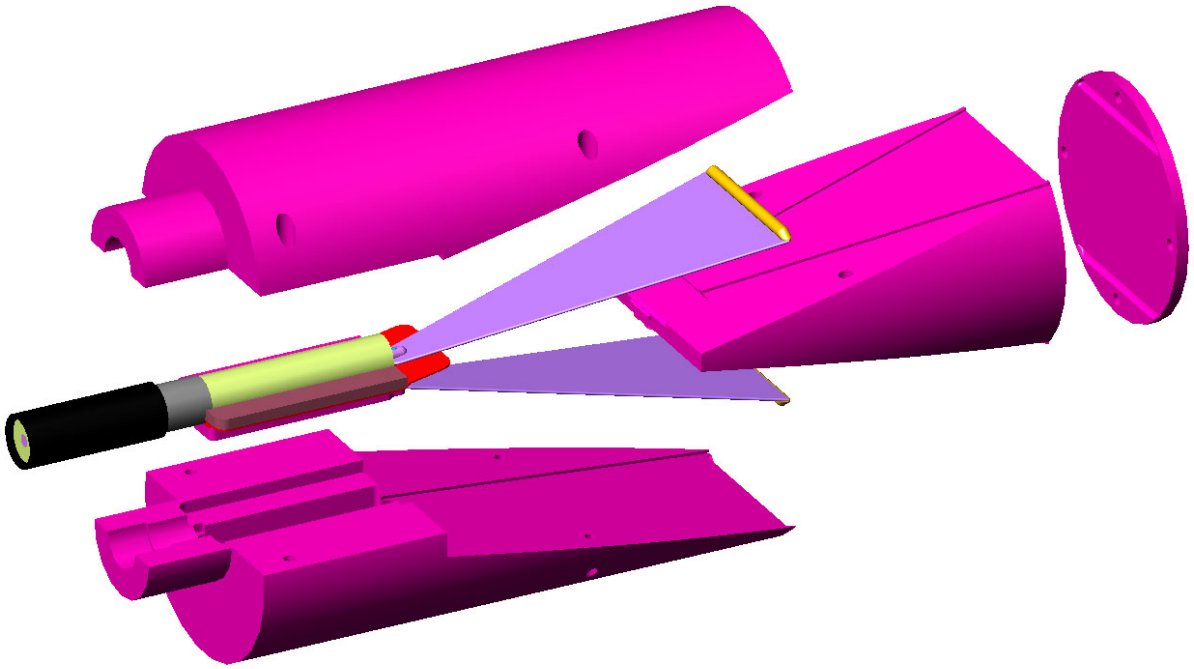

Figure 2.3. The SDL-3 with Kynar® filling shown all in the same color.

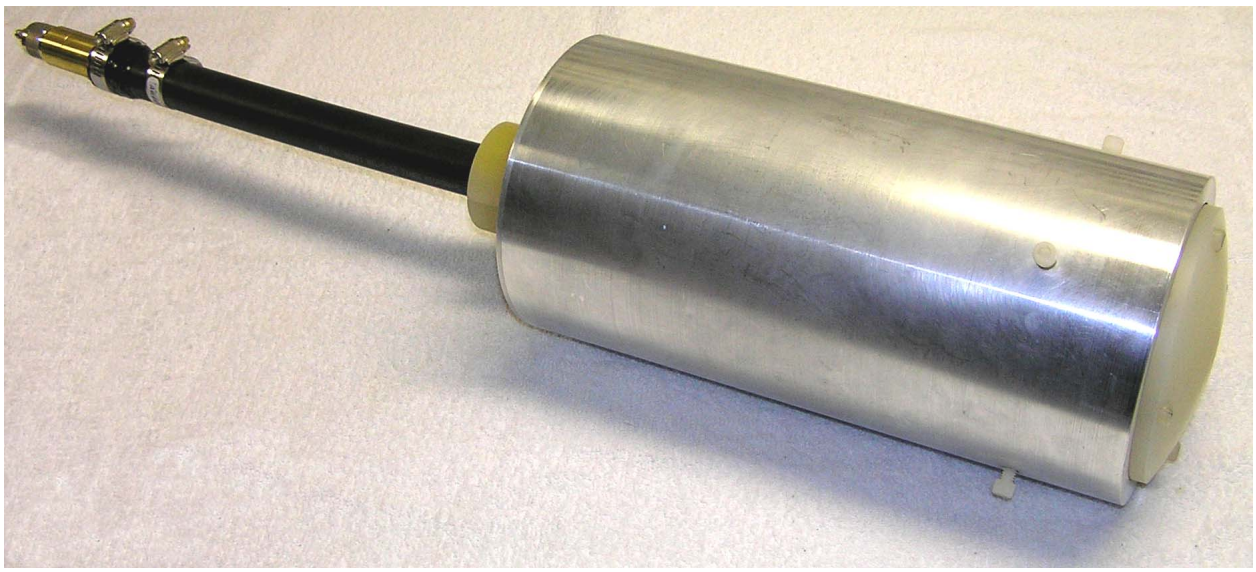

Figure 2.4. The SDL-3 with RG-220 cable and with shroud in flush position.

In the aperture of the SDL-3 is a lens in the shape of a prolate spheroid, or an ellipse of revolution. The lens is fabricated from the same Kynar® material as the rest of the dielectric filler. The design calculations for the lens of the SDL IRA come from [6]. The lens is an ellipse of revolution with a major axis of 2*a* and a minor axis of 2*b* where

$$a = \frac{L}{1 + \frac{1}{\sqrt{\varepsilon_r}}} \tag{2}$$

$$b = L\sqrt{\frac{\sqrt{\varepsilon_r} - 1}{\sqrt{\varepsilon_r} + 1}} \tag{3}$$

and

$$\frac{b}{a} = \sqrt{1 - \frac{1}{\varepsilon_r}} \tag{4}$$

In these equations, L is the distance from the feed point to the end of the lens and ε_r is the relative dielectric constant of the lens. Once a and b are calculated for the specified L and ε_r, then the shape of the lens can be calculated from the standard formula for an ellipse. In this case, the ellipse of rotation was approximated by a spherical surface covering the aperture of the horn. In [1] we experimented with removing the lens and found that it was best to use the lens. Therefore, for the measurements made here the lens is always in place.

The SDL-3 is fed by a length of RG-220 cable, which has an operating voltage of 14-kV DC. We have previously used RG-220 for fast transients with peak voltages of around 120 kV.

III. NUMERICAL MODELLING.

We used CST's Microwave Studio to model the SDL-3 and the HiZ antenna described in [1]. We did so in order to determine whether we expect the higher dielectric constant of the SDL-3 to improve performance. Microwave Studio is a Finite Volume Time Domain code that can analyze a 3D problem space on a conformal grid. We studied how the Lens IRA performs as a function of several variables, including antenna length, dielectric constant, and antenna position with respect to the shroud.

We analyzed the two antennas over a frequency range of 0-10 GHz. In our models, all metals are lossy. We replaced the coaxial feed with a stripline feed of length 5 cm (2 in.) to simplify the calculation. We applied the excitation voltage as a multi-pin waveguide port at the far end of the stripline with the top plate as a positive voltage, the bottom plate as the negative voltage, and the conducting shroud as the ground. We selected a meshing that was 7 cells per wavelength at 10 GHz. This resulted in 1.25 million cells with Kynar® and 500 thousand cells with UHMW. The boundary conditions were an open boundary using CST's Perfectly Matched Layers (PML). A sketch of the configuration that was modeled is shown in Figure 3.1.

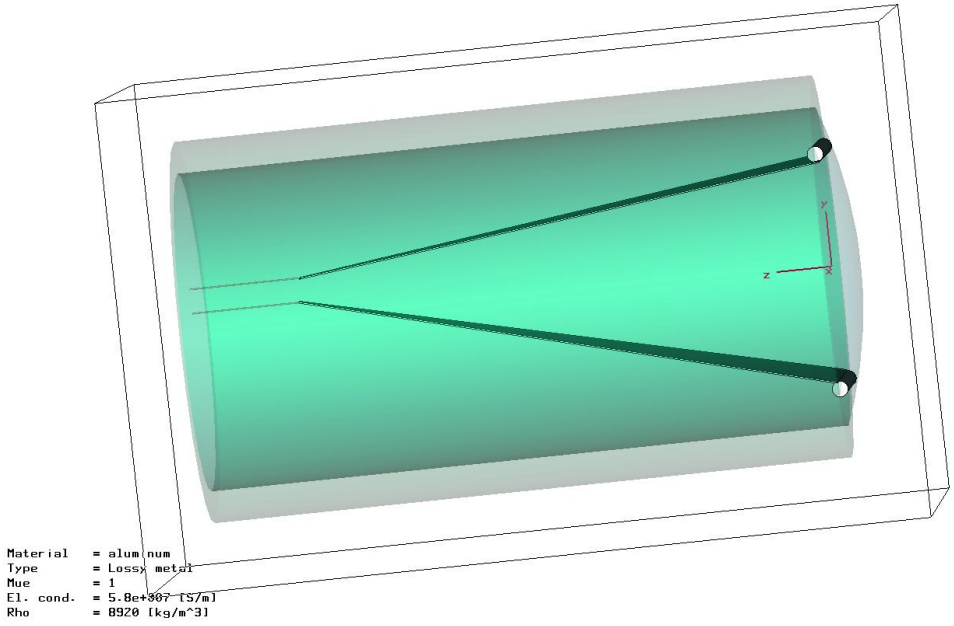

Figure 3.1. A solid model of the SDL IRA using a stripline feed.

To obtain the radiated far field on boresight, we placed a far-field probe outside of the PML boundary at a position 22.9 cm (9 in.) in front of the aperture. We maintained the same position for all the shroud positions. The excitation signal was a step-like function with 30 ps risetime, 10 ns hold time and 5 ns fall time.

We plot the radiated field on boresight for the SDL-3 in Figure 3.2. We overlay the results of five antenna positions with respect to the shroud in 5 cm increments. These positions vary in 5 cm increments from antenna protruding 10 cm (far left) to antenna receded within the shroud by 10 cm (far right). We observe a significant variation with respect to antenna position.

We plot the Fourier transform of this result in Figure 3.3, where we observe improved low-frequency response for the antenna positions that protrude further.

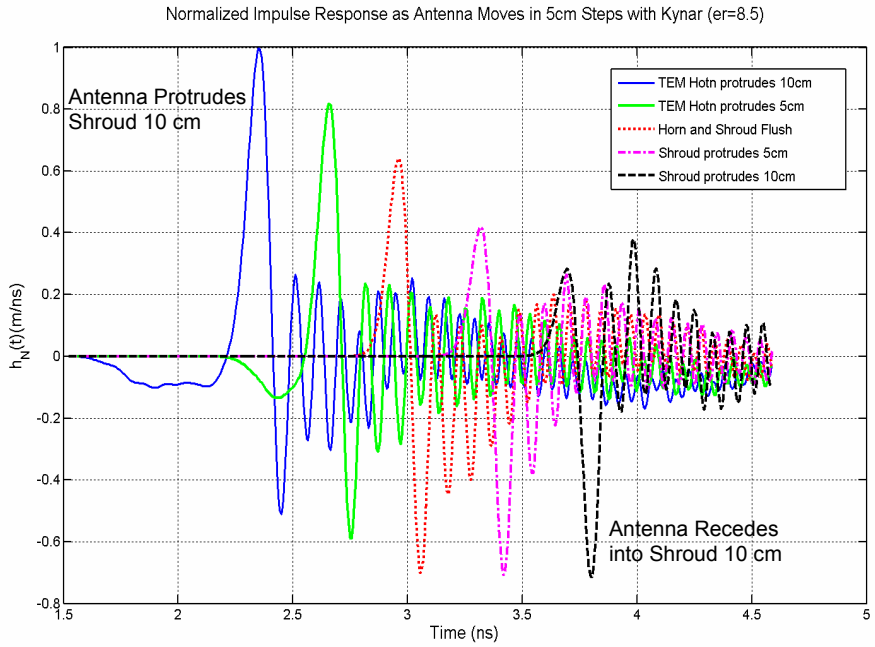

Figure 3.2. Response of the SDL-3 in the time domain as a function of antenna position with respect to the shroud, in 5-cm increments.

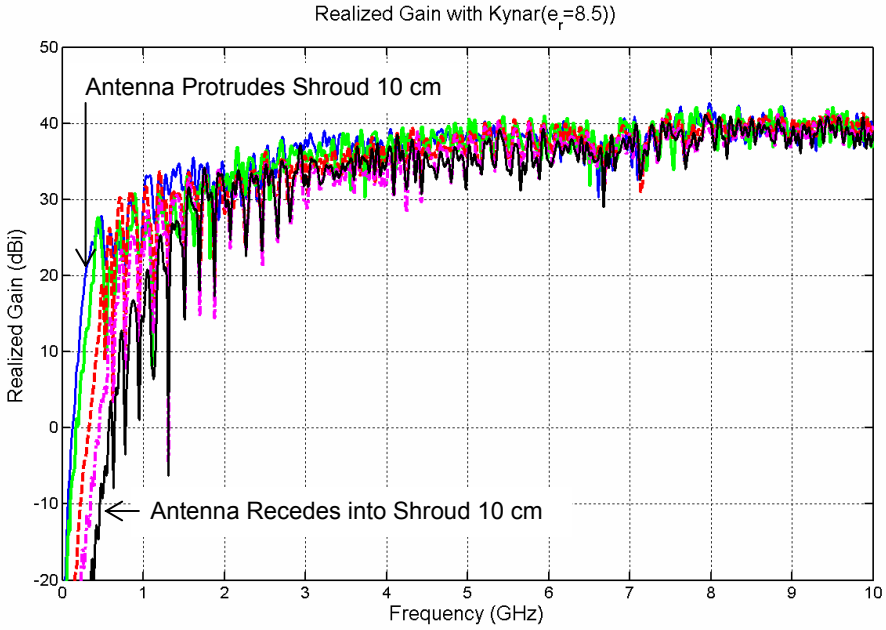

Figure 3.3. Response of the SDL-3 in the frequency domain as a function of antenna position with respect to the shroud, in 5-degree increments.

Next, we compare the impulse response of the SDL-3, filled with Kynar, to that of the HiZ configuration, filled with UHMW polyethylene, as shown in Figure 3.4. These impulse responses were calculated with the front of the antennas flush with the shroud, so this is not quite the optimal configuration. Nevertheless, we observe that the impulse response of the HiZ configuration is has a higher peak and is more well-behaved. We convert the impulse response to realized gain in Figure 3.5, where we observe that the HiZ configuration tends to have a better response over most of the frequency range, but the SDL-3 has a better realized gain at low frequencies.

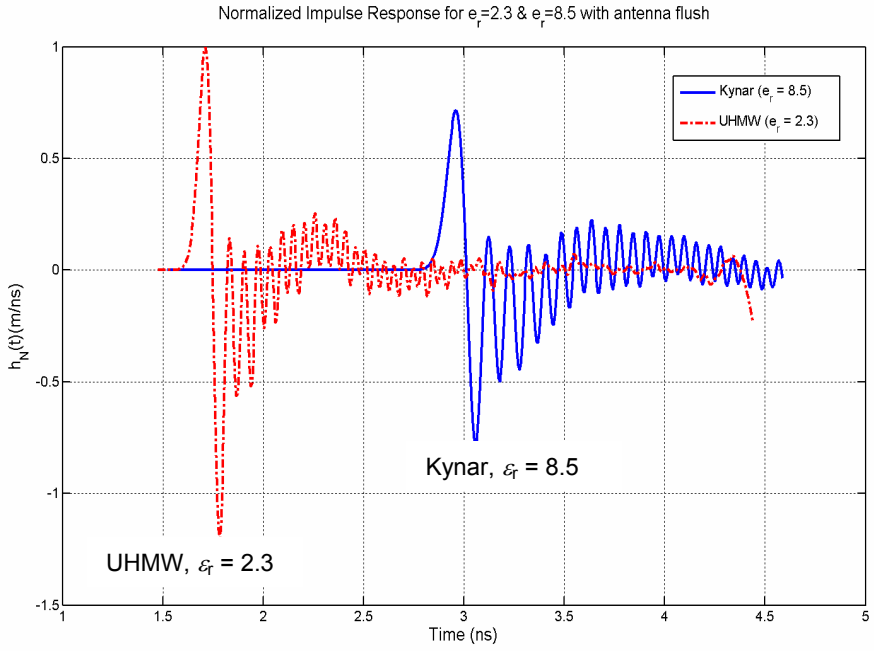

Figure 3.4. Predicted impulse response of the HiZ configuration (filled with UHMW, left) and for the SDL-3 (filled with KYNAR, right), with both antennas flush to the shroud.

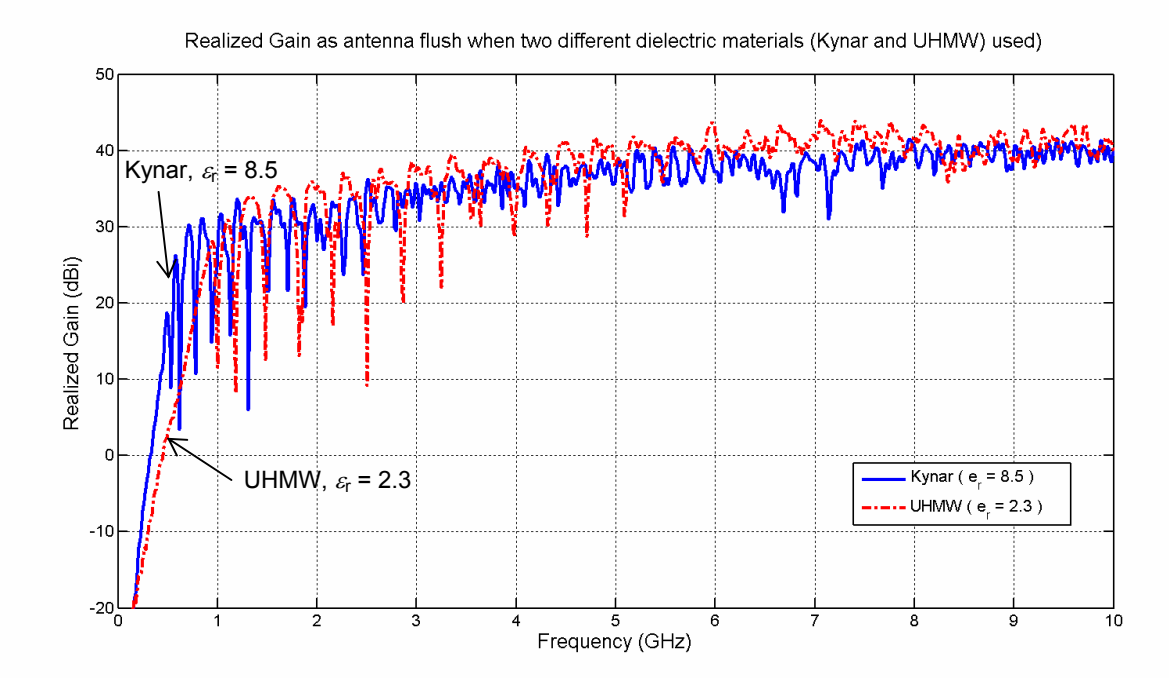

Figure 3.5. Predicted realized gain of the HiZ configuration (filled with UHMW, dashed) and for the SDL-3 (filled with KYNAR, solid), with both antennas flush to the shroud.

IV. TEST DATA.

We begin the test data with the TDR of the antenna, as shown in Figure 4.1, where we show the TDR both with and without the shroud. The solid line (bottom) is the TDR with the shroud positioned so that its front edge is flush with the aperture of the horn, i.e. flush with the ends of the feed elements. The top line (dashed) is the TDR with the shroud removed.

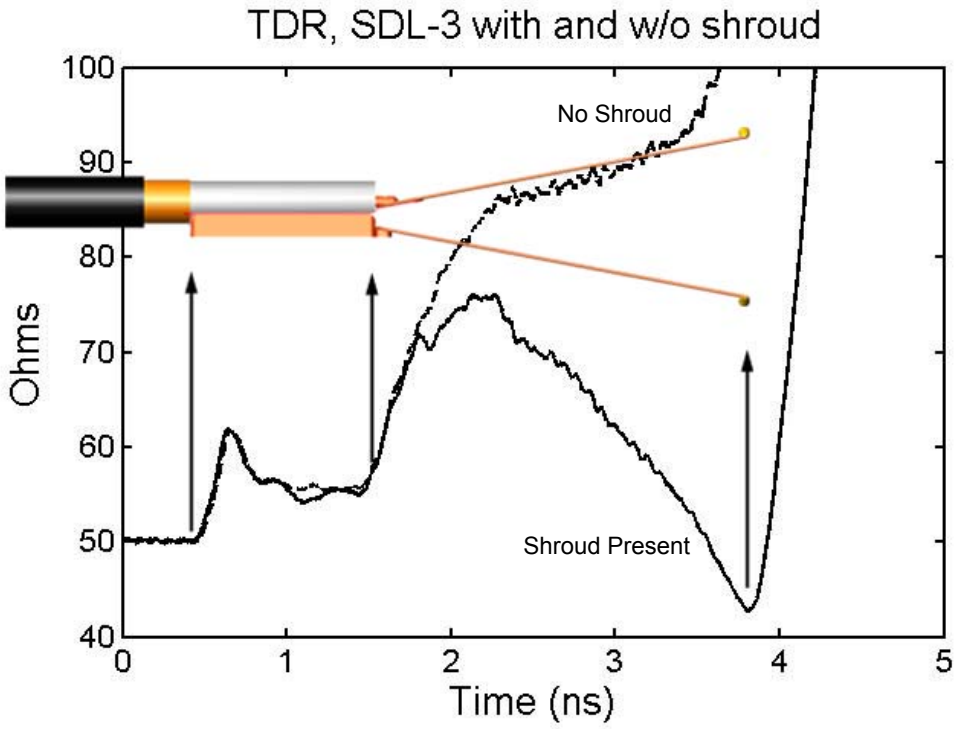

Figure 4.1 TDR of the SDL-3 with and without the aluminum shroud.

We tried to design the SDL-3 so that the impedance would be 50 Ω up to the feed point of the horn (second arrow). However, the jump in the impedance at the end of the braid (first arrow) is higher than we would like and the impedance between that point and the feed point is higher than calculated. The formula used for this calculation assumes that the diameter of the wire is much less than its height above an infinite ground plane. In this case the height is about the same as the diameter and the ground plane is narrow, so the calculation is only approximate at best. Also, the center conductor of the RG-220 is not accurately centered in the insulation, so there are several sources for possible error. We may be able to improve the impedance match by modifying some of the parts used in this area. From the feed point to the end of the horn the impedance should increase from 50 Ω to about 61 Ω. We wanted the aperture of the horn to be as large as possible and still fit inside the shroud. At the aperture the feed elements are quite close to the inside surface of the shroud, so the impedance drops at this point (third arrow) when the shroud is present.

At the aperture of the horn the impedance was calculated to be approximately 61 Ω based on the width and separation of the feed elements and on a relative dielectric constant of 8.5. We

would like for the dielectric constant to be this high at all frequencies but that is not the case. The manufacturer of the Kynar® used to construct the SDL-3 lists the dielectric constant as 8.5 at 1 MHz. Other manufacturers list the dielectric constant as 9 at 60 Hz and 6.1 at 1 MHz. No specifications were available in the GHz range, which is the primary range of interest in this experiment. If we calculate the dielectric constant based on an impedance of around 90 Ω as we see at the end of the feed elements in Figure 4.1, we get approximately 4.

The antenna measurements were made using our newly developed Portable Automated Time-domain Antenna Range (*PATAR*™) System. The system includes a fast pulser, a fast digital sampling oscilloscope, two calibrated TEM field sensors, an elevation/azimuth antenna positioner, a computer controller, and software for system control, data acquisition, and data processing. The pulser is a PSPL model 4015C with a rise time of approximately 20 ps. The pulser drives one of the TEM sensors to form the transmit portion of the antenna range. The oscilloscope is a Tektronix model TDS8000 with an 80E01 sampling head. The SDL-3 is connected to the TDS8000 to form the receive section of the system. The antenna positioner has a non-conductive mast that supports the antenna under test approximately 3 m above the ground. The distance between the apertures was 10 m for the test with the antenna in the flush configuration and 7 m where the antenna protruded 10 cm in front of the shroud.

We consider now the effect of the shroud position. To do this we first recessed the horn aperture 10 cm inside the shroud and then moved the antenna out in 5 cm steps until it protruded 15 cm in front of the shroud. The results are shown from right to left in Figure 4.2, where the numbers indicate the distance that the aperture protrudes in front of the shroud. When we compare this figure to Figure 4.9 in [1], we see that the peak of the impulse response is more uniform than for the HiZ antenna filled with polyethylene. In that case, the peak of the impulse response showed a definite increase as the antenna was moved from the –10 cm position to the +10 cm position. We expected to the same variation for the SDL-3, but the shroud position does not make as much difference in this case. Also, the impulse response for the HiZ antenna was strongly double peaked. The impulse response for the SDL-3 has a better shape, but the peaks are not as high. This leads to the lower gains shown in Figure 4.3.

The flush (+0) and +10 cm configurations were chosen for more thorough study, as we will see later in this section. The data from these configurations can be compared directly to the data presented in [1]. The +15 cm case has about the same peak value as the +10 cm case, so there is little reason to extend the antenna that far in front of the shroud. Also, the impulse response begins to have a more double peaked shape as the antenna protrudes further in front of the shroud.

We consider now how well we have achieved our intended goal of improving the low frequency response by using a high dielectric material. In Figure 4.3, we observe an improvement in the response between 100 and 300 MHz, but it is unclear how accurate our measurements are at these low frequencies. In the frequency ranges of 0.3–1.0 GHz and 2–8 GHz the response of the SDL-3 is actually lower than of the HiZ design. It therefore seems that we have not met our objective in using the higher dielectric material.

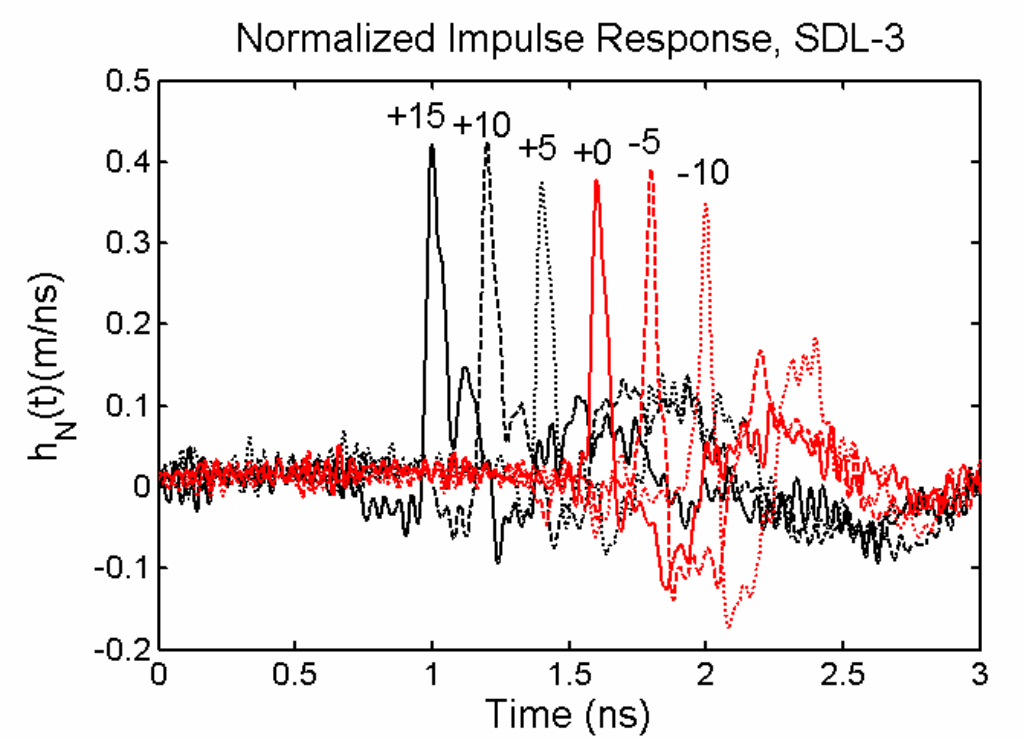

Figure 4.2 Normalized impulse response of the SDL-3 with the shroud in 6 positions.

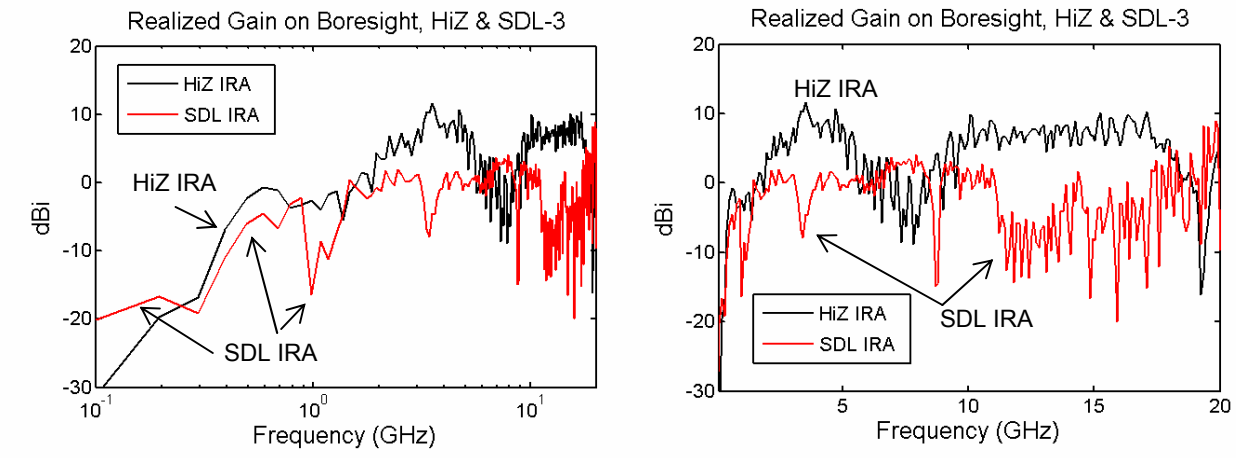

Figure 4.3 Realized gain for the HiZ antenna [1] and the SDL-3 both with the antenna protruding 10 cm in front of the shroud.

Next, we consider the effect of having the antenna protrude beyond the shroud. In Figure 4.4 we compare the realized gains of the SDL-3 with the aperture flush to the shroud and protruding 10 cm. We observe a big improvement in realized gain below 1 GHz, when the aperture protrudes 10 cm. We also see in Figure 4.4 a number of strong dips in the realized gain near 1 GHz, 4 GHz, and 8.5 GHz. The HiZ antenna had a dip in gain at the last frequency, but the dip for the SDL-3 is deeper and much sharper.

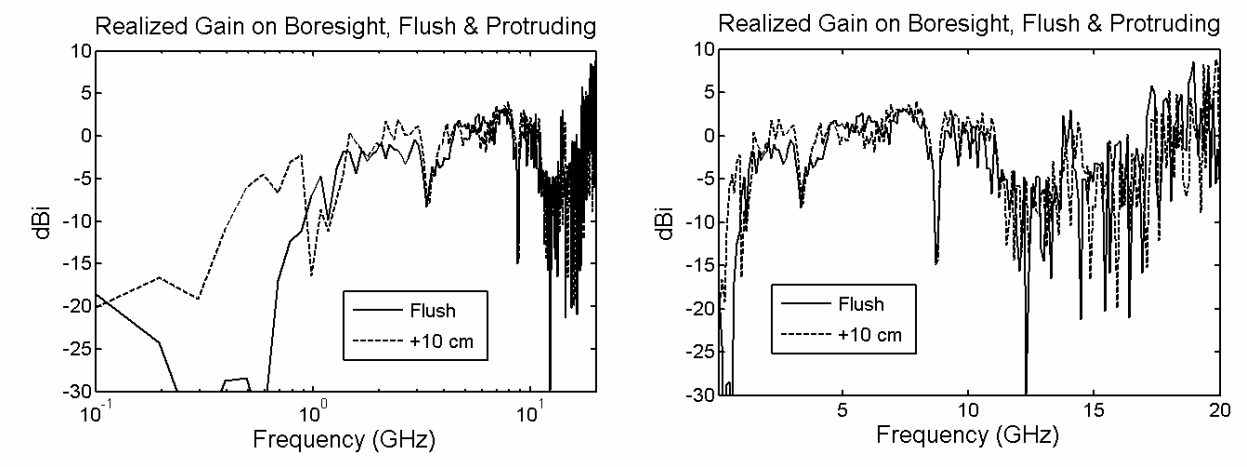

Figure 4.4 Realized gain with the shroud flush and back 10 cm.

Now we provide more detailed data for the case with the aperture flush with the front of the shroud. Later we show similar data for the case with the aperture 10 cm in front of the shroud. In Figure 4.5 we show the SDL-3 mounted on the *PATAR*™ antenna positioner. For the low voltage tests, an SMA adapter is use to facilitate connection between the HN-type connector on the RG-220 cable and the sampling head of the digital oscilloscope.

Figure 4.5 The SDL-3 with horn aperture flush with the front of the shroud.

In Figure 4.6 we show the TDR of the SDL-3 in the flush configuration. This TDR was also shown in Figure 4.1 without the connectors and adaptors at the end of the RG-220, which appear to the left in this figure. The TDR of the antenna shows that it is not as well matched to 50 Ω as we would like. The impedance at the aperture of the horn should be about 61 Ω as mentioned earlier but in this case it drops rather drastically due to the presence of the aluminum shroud.

The impulse response shown in Figure 4.7 has a reasonably good shape in that it does not have the double peak that is characteristic of the antennas described in [1]. There is an undershoot that occurs after the main pulse, but this might be considered to be less of a problem because it is broad. However, the peak is lower so the gains as shown in Figure 4.8 and 4.9 are not as high as those reported in [1].

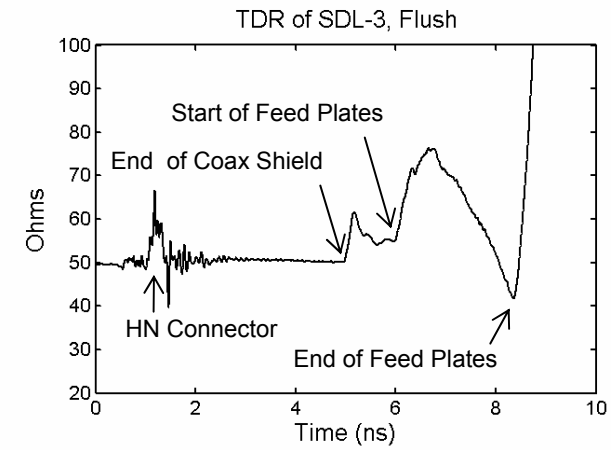

Figure 4.6 TDR with the shroud flush.

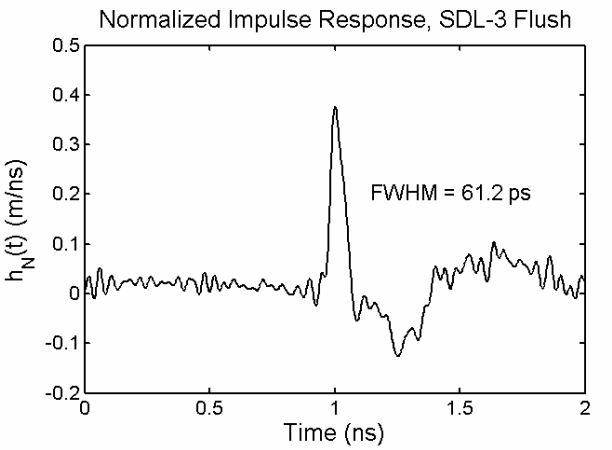

Figure 4.7 Normalized impulse response.

There are several noticeable features about the plots in Figures 4.8 and 4.9. First the realized gain at the low end is not as good as we had hoped it would be by using the high dielectric constant material. Next, there is a dip in the gain between 3.5 and 4.5 GHz. Finally, there is a sharp dip at about 8.5 GHz. There was also a dip around 8.5 GHz for the low dielectric HiZ antenna but it was not as sharp. As yet we have not determined the reason for this dip. There is some difference between the realized gain and the standard gain, but it is not great.

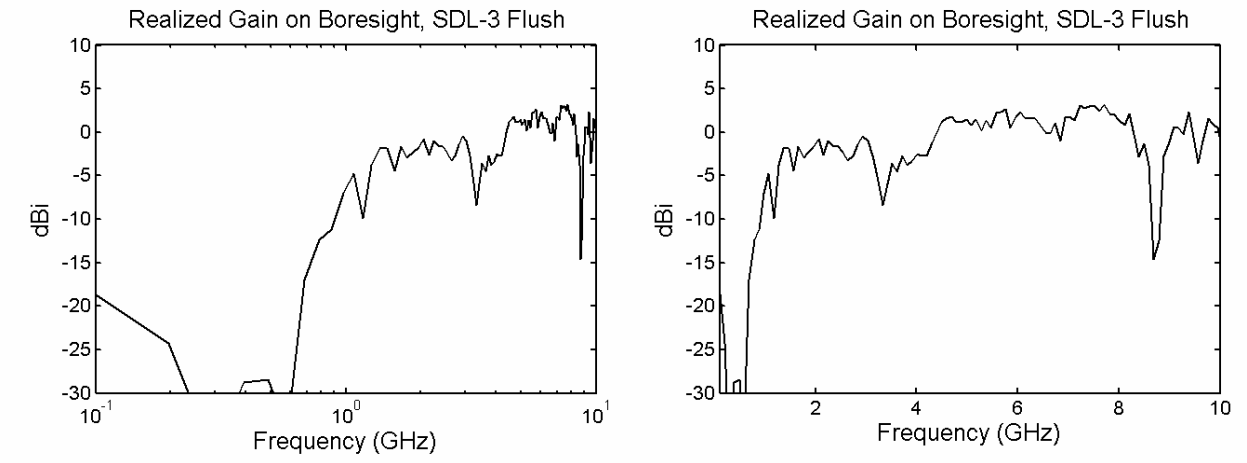

Figure 4.8 Realized Gain on boresight with the shroud flush with the aperture.

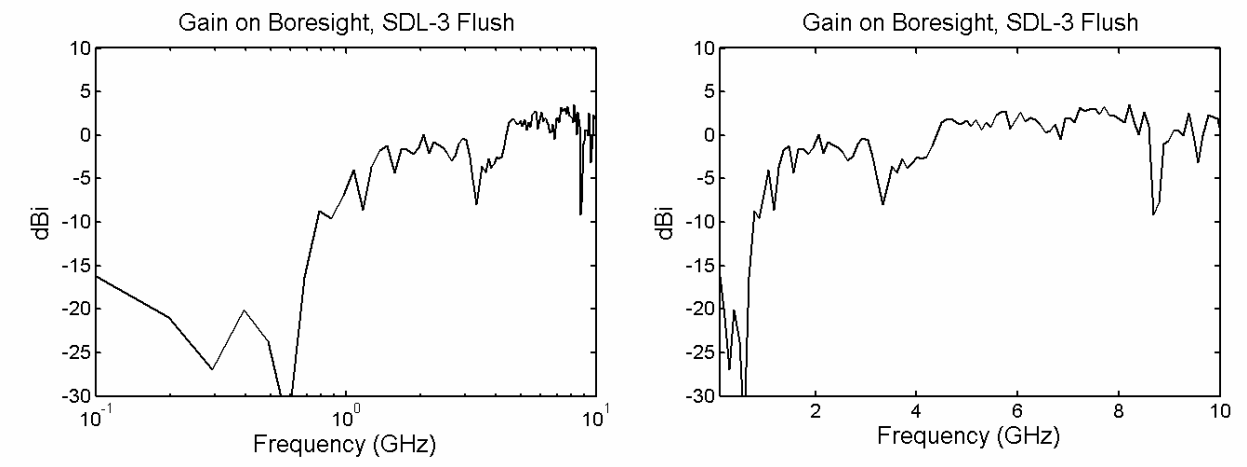

Figure 4.9 Gain on boresight with the shroud flush with the aperture.

In Figure 4.10 we show the patterns in the H and E planes for the SDL-3. These patterns are based on the peak value of the normalized impulse response. The pattern in the H plane (azimuth) is symmetrical about physical boresight or the axis of symmetry. However, the peak E field occurs at about 5° below boresight in the E plane (elevation). The pattern measurements were made in 1° increments from -30° to +30° off boresight.

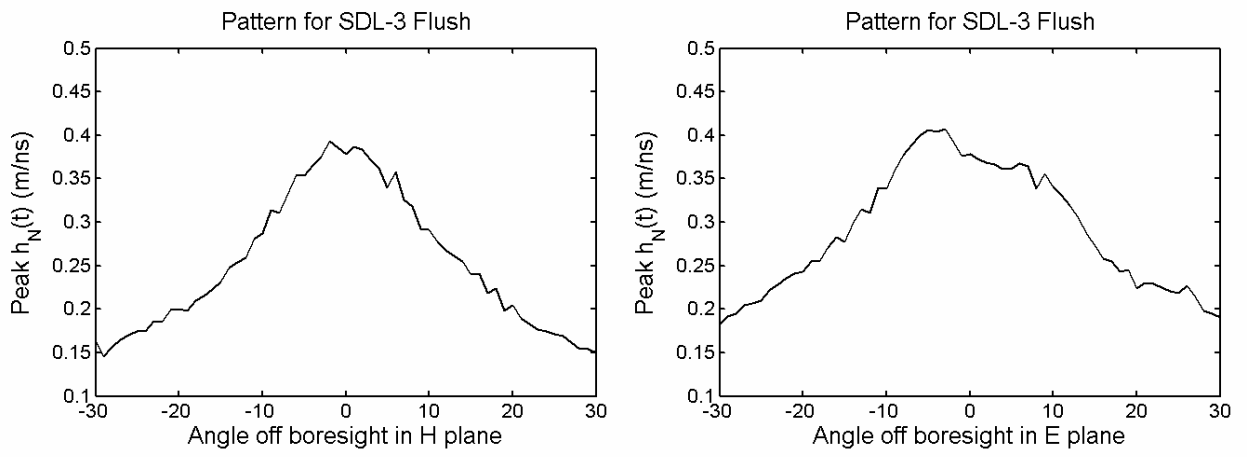

Figure 4.10 Antenna patterns based on the peak of the normalized impulse response.

The antenna patterns normalized to the gain on boresight are shown in Figure 4.11. In these plots, the normalized gain is plotted as a function of the angle off boresight and frequency. Above 10 GHz the gains become rather noisy.

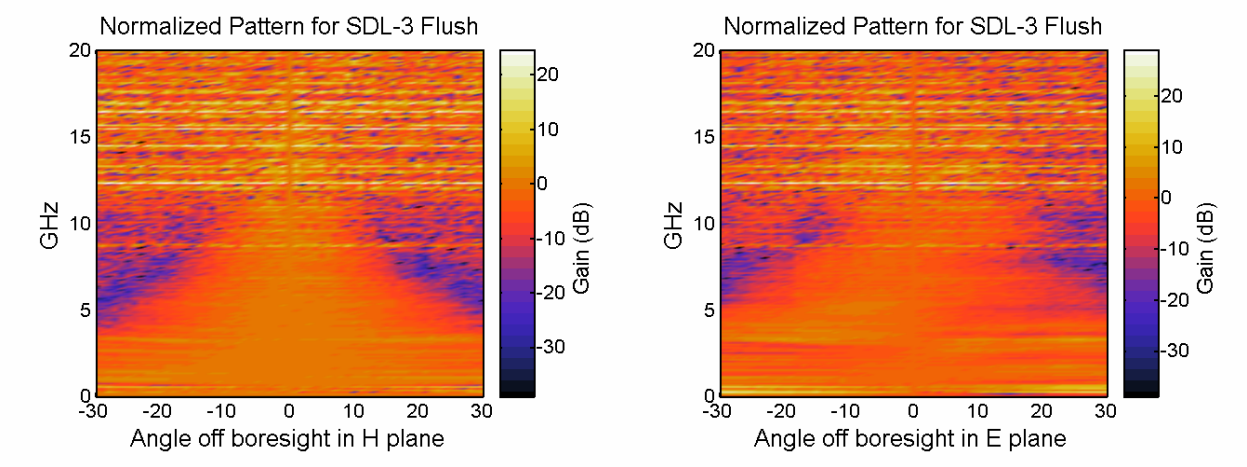

Figure 4.11 Gain as a function of frequency and angle in the H and E planes.

The last set of data is for the SDL-3 with the aperture protruding 10 cm in front of the aluminum shroud as shown in Figure 4.12. In this picture the antenna is mounted on the *PATAR*™ antenna positioner. The +10 cm configuration gives better results than the flush case because the conductive shroud is not as close to the feed elements of the horn near the aperture.

Figure 4.12 SDL-3 with horn aperture 10 cm in front of the shroud.

In Figure 4.13 we show the TDR of the antenna in the above configuration. The impedance of the horn dips somewhat when the feed elements approach the shroud and then goes toward infinity at the end of the horn.

The normalized impulse response of the antenna is shown in Figure 4.14. In this plot we see that a second peak is beginning to appear. A double peaked impulse response was characteristic of the HiZ antenna reported in [1].

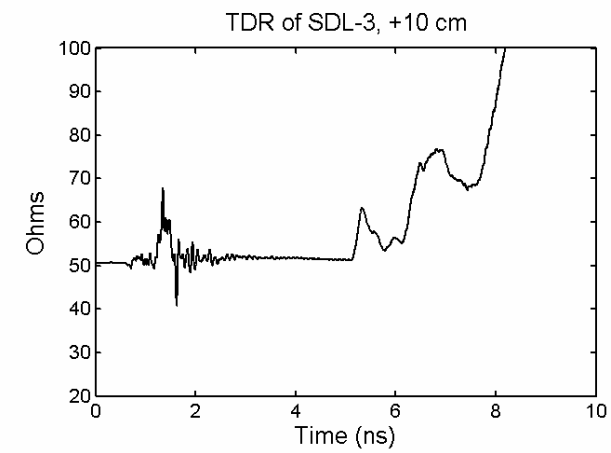

Figure 4.13 TDR with the shroud back 10 cm.

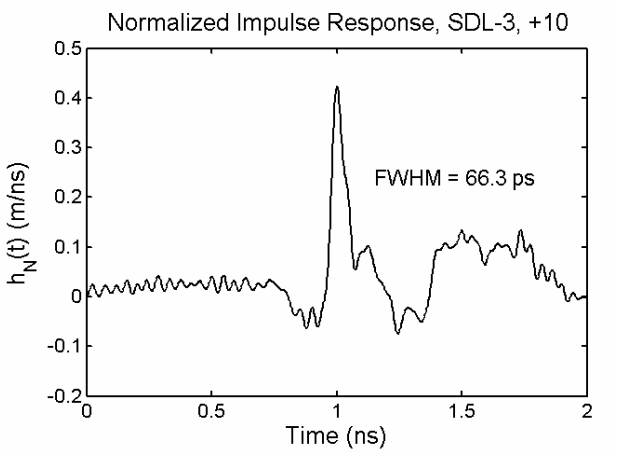

Figure 4.14 Normalized impulse response.

In Figures 4.15 and 4.16 we show the realized and standard gain for the configuration with the antenna protruding 10 cm in front of the shroud. In this configuration we see that the gain at the low end is greatly improved but it is still not much better than the HiZ antenna reported in [1]. We also see that the dips at 1 – 1.6 GHz, 3.5 – 4.5 GHz and at 8.5 GHz are still very evident.

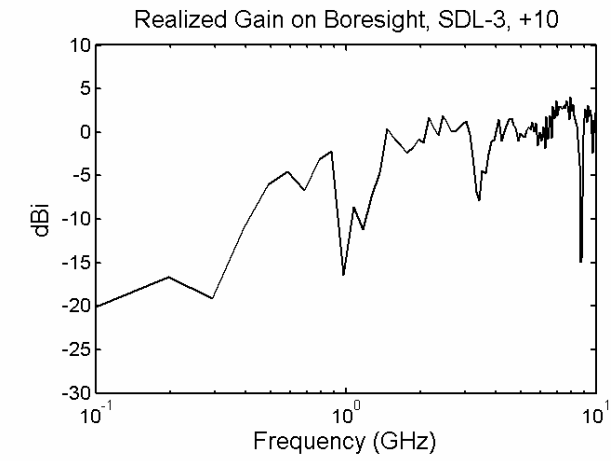

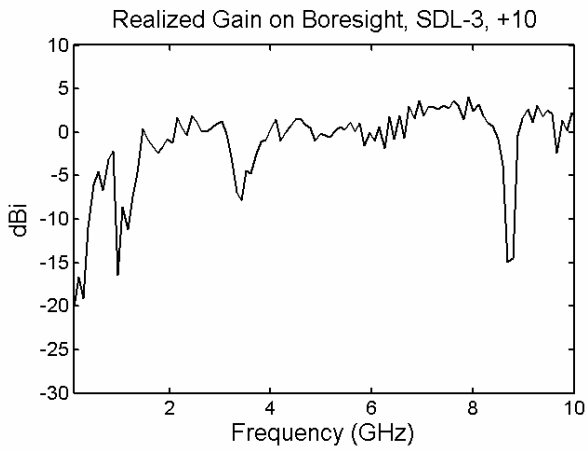

Figure 4.15 Realized Gain on boresight with the shroud 10 cm behind the aperture.

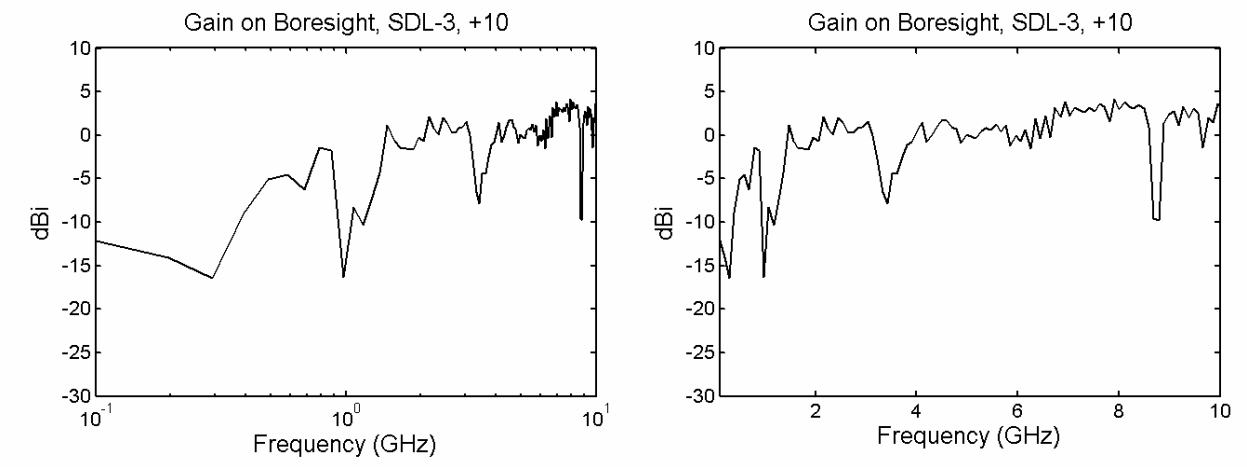

Figure 4.16 Gain on boresight with the shroud 10 cm behind the aperture.

In Figure 4.17 we show the pattern plots based on the peak value of the normalized impulse response. As in Figure 4.10, we see that the pattern is very symmetric about physical boresight in the H plane and not so symmetric in the E plane. The pattern is rather flat in the E-plane.

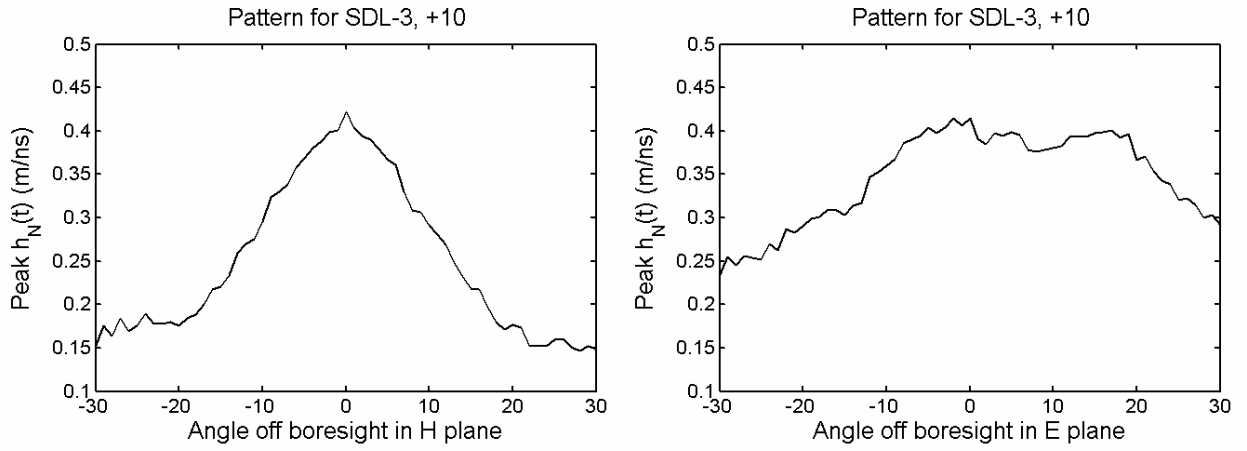

Figure 4.17 Antenna patterns based on the peak of the normalized impulse response.

Finally we show the normalized gain versus frequency and angle off boresight in Figure 4.18. Again the gains above 10 GHz are rather noisy.

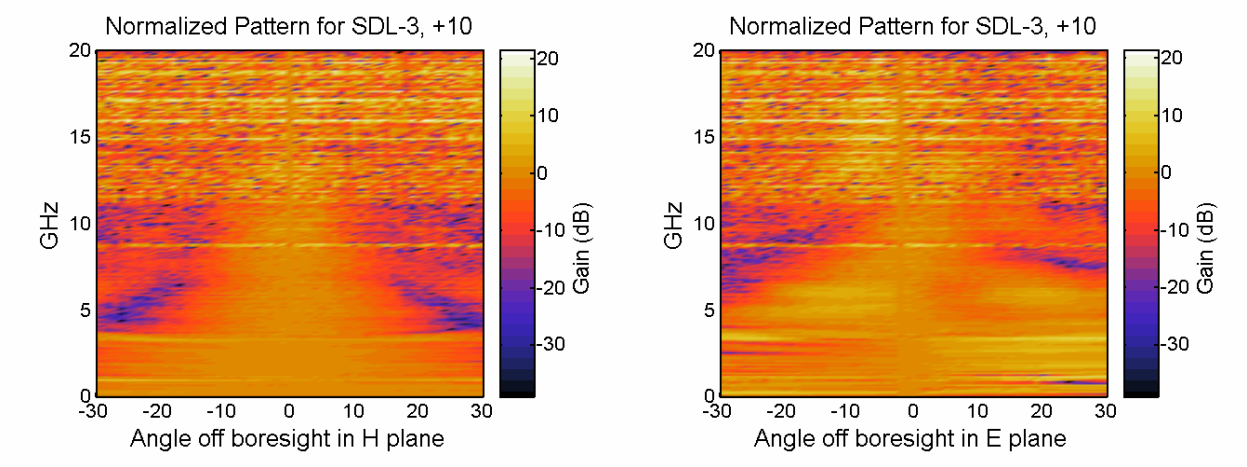

Figure 4.18 Gain as a function of frequency and angle in the H and E planes.

Finally, we tested the SDL-3 at high voltage using a 17 stage Marx generator with a rated output of 120 kV. This device was characterized earlier in [7]. After a few shots, we determined that the antenna was arcing internally so the test was discontinued. The SDL-3 was then disassembled to determine the location of the arcing. We found that the breakdown was through the 2 layers of high quality UHMW separating the conductors at the transition between the feed cable and the TEM horn. The gap at the feed point of the TEM horn is very narrow in this design so 2 layers of high quality UHMW were inserted in this area to improve the high voltage standoff. Based on Table 2.1, the layers of UHMW which total 1 mm (0.04 in.) should be able to withstand about 91 kV. This is below the applied voltage of 120 kV, but the pulse duration was short, so we expected to be able to exceed the specifications for low frequency or DC ratings.

To improve this antenna, we need to redesign the antenna to have a better impedance match in the transition between the cable and the TEM horn. This will require, among other things, a wider gap between the conductors. We would also modify one copper part in the transition by making it thinner and rounding the edges. An additional layer or two of the UHMW could also be used to help improve the high voltage standoff.

V. DISCUSSION.

We expected that using a material with a high dielectric constant would improve the performance of the SDL-3, because it increased its electrical length. While we obtained some improvement in our experimental model below 300 MHz, the performance above 300 MHz was worse overall than that of the HiZ version described in [1]. Furthermore, we note that below 300 MHz it is difficult to assess the accuracy of our measurement system. Our numerical modeling generally supports these results.

Our idea that a higher dielectric constant should improve performance seemed to be supported by Scheers and Yarovoy [3, 4], who found improved low-frequency performance in dielectric-filled TEM horns when compared to those filled with air. However, they compared the performance of horns filled with dielectric (ε_r = 2.8) and air, while we compared versions filled with Kynar® and polyethylene. Furthermore, the TEM structures of [3] and [4] had shaped feed elements, instead of simple triangular patches used here. Finally, the antennas in [3] and [4] were designed for ground penetrating radar and mine detection, so their measurement techniques and criteria for success were somewhat different than ours.

One reason for the modest performance of the SDL-3 may be the material properties of the filler material. The Kynar® used here had the best characteristics of any PVDF (PolyVinyliDene Fluoride) that we could find. However, the specifications for PVDF vary drastically in the literature, and we did not measure them ourselves. One source specifies Kynar® with a dielectric constant of 8.5 and loss tangent of 0.05 at 1 MHz. Another source specifies the dielectric constant and dissipation factor for PVDF at 1 MHz as 6.0 and 0.153 respectively. The characteristics of most dielectrics vary considerably with frequency and there are usually no data available in the literature at frequencies in the GHz range.

Another factor contributing to the modest performance of the SDL-3 is impedance mismatch at the horn feed, as is apparent from the reflections in the TDR. With some experimentation, these TDRs can be made more smooth.

There are several dips in the realized gain of the SDL-3 for which we have not determined a cause. These dips occurred at 1 - 1.6 GHz, 3.5 - 4.5 GHz, and 8.5 GHz and were of various depths and widths. It is interesting that all three of the antennas studied here and in [1] had a dip in the realized gain at 6 - 9 GHz. Since this dip occurs at a lower frequency for the LoZ antenna, it would seem that it is not due to the measurement methods or equipment. Also, since it occurs at the same frequency for both of the high impedance antennas, with two different dielectric materials, it is probably not due to the dielectric.

We tested the SDL-3 antenna with the horn at various locations within the shroud, and found that the best configuration had the horn protruding 10 cm in front of the shroud. This gets the conductive shroud away from the aperture of the horn so it interferes less with the fields generated within the horn and propagated from the aperture. As the antenna protrudes further in front of the shroud, the gain at low frequencies improves considerably. However, in doing so, the impulse response developed a second peak. Also, the pattern in the vertical plane became flatter and less symmetrical about boresight.

Future work on the SDL-3 would encompass a number of areas. First, we would smooth the TDR to improve the impedance match. Hopefully this would also eliminate the dips in the gain mentioned in the previous paragraph. We would also add another layer of UHMW to prevent arcing at high voltage. It would also be useful to explore reshaping the feed elements of the horn to make them similar to those of [3] and [4]. It is unclear that Kynar® is the best material to use in future versions, since the HiZ version in [1] that was filled with UHMW polyethylene performed much better. Additional work is also needed to ruggedize the antenna to withstand high g-forces.

VI. CONCLUSIONS AND RECOMMENDATIONS.

We built and tested a Solid Dielectric Lens Impulse Radiating Antenna, the SDL-3, which has a TEM horn embedded into a material with a high dielectric constant ($\varepsilon_r \approx 8.5$). The antenna was designed to fit inside a cylindrical conductive shroud. This work extended earlier work on SDL IRAs by using a higher-dielectric material instead of polyethylene.

The intent of using a material with a higher dielectric constant was to increase the electrical size of the horn to improve its low frequency response. It was hoped that this would improve the response over that of the HiZ version reported in [1]. We found in both our numerical and experimental models that low-frequency performance was indeed improved. In our experiments we observed improved realized gain in the SDL-3 below 300 MHz, but we note that our measurement technique is only approximate in this frequency range. Above 300 MHz, the new antenna had a realized gain that was either comparable to or worse than that of the HiZ antenna. These results were supported by numerical simulations using CST's Microwave Studio.

While there are some improvements to the SDL-3 that we can try near the feed point, it seems unlikely that the high dielectric material is an advantage in the design of SDL IRAs. The next step in the development of SDL IRAs is probably to return to a design filled with UHMW polyethylene and shape the feed elements as described in [3, 4].

REFERENCES

1. E. G. Farr, L. M. Atchley, D. E. Ellibee, and L. L. Altgilbers, A Solid Dielectric Lens Impulse Radiating Antenna Surrounded by a Cylindrical Shroud, Sensor and Simulation Note 487, March 2004.
2. E. G. Farr, et al, Development of a Reflector IRA and a Solid Dielectric Lens IRA, Part II: Antenna Measurements and Signal Processing, Sensor and Simulation Note 401, October 1996.
3. B. Scheers, M. Piette, A. Vander Vorst, Development of dielectric-filled TEM horn antennas for UWB GPR, Millennium Conference on Antennas & Propagation AP-2000, April 9-14, 2000, Davos, Switzerland, Vol. II, pp. 187.
4. A. G. Yarovoy, A. D. Schukin, I. V. Kaploun, and L. P. Ligthart, The Dielectric Wedge Antenna, IEEE Transactions on Antennas and Propagation, Vol. 50, No. 10, October 2002.
5. E. G. Farr and C. E. Baum, A Simple Model of Small-Angle TEM Horns, Sensor and Simulation Note 340, May 1992.
6. E.G. Farr and C.A. Frost, Development of a Reflector IRA and a Solid Dielectric Lens IRA, Part I: Design, Predictions, and Construction, Sensor and Simulation Note 396, April 1996.
7. E. G. Farr, L. M. Atchley, D. E. Ellibee, W. J. Carey, and L. L. Altgilbers, A Comparison of Two Sensors Used to Measure High-Voltage, Fast-Risetime Signals in Coaxial Cable, Measurement Note 58, March 2004.